THE JOURNAL OF COMPARATIVE NEUROLOGY 366:244–258 (1996)

Regional Distribution of Cytochrome P450 2D1 in the Rat Central Nervous System

P.J. NORRIS, J.P. HARDWICK, AND P.C. EMSON
MRC Molecular Neuroscience Group, Department of Neurobiology, The Babraham Institute, Babraham, Cambridge, CB2 4AT, United Kingdom (P.J.N., P.C.E.); Department of Biochemistry, NEOUCOM, Rootstown, Ohio 44272 (J.P.H.)

ABSTRACT

Cytochrome P450s are enzymes involved in the oxidative metabolism of numerous endogenous and exogenous molecules. The enzyme cytochrome debrisoquine/sparteine-type monoxygenase is a specific form of cytochrome P450 and is found in the liver and the brain (in the rat the enzyme is known as CYP2D1). CYP2D1 has no established role in the brain; however, it has been shown to share substrate and inhibitor specificities with the dopamine transporter and the enzyme monoamine oxygenase B. Using CYP2D-specific deoxyoligonucleotide probes and a polyclonal antibody to CYP2D1, we have mapped the distribution of CYP2D mRNA and CYP2D1-like immunoreactivity in the rat central nervous system.

CYP2D1 immunoreactivity and the CYP2D mRNA signal were heterogenously distributed between brain areas. There were moderate to high levels of immunoreactivity and mRNA signal in the olfactory bulb, olfactory tubercle, cerebral cortex, hippocampus, dentate gyrus, piriform cortex, caudate putamen, supraoptic nucleus, medial habenula, hypothalamus, thalamus, medial mamilliary nucleus and superior colliculus. In the brainstem, strong CYP2D1 immunoreactivity and CYP2D mRNA signal were observed in the substantia nigra compacta, red nucleus, interpeduncular nucleus, pontine grey, locus coeruleus, cerebellum, and the ventral horn of the spinal cord.

This study indicates that CYP2D1 is widely and constitutively expressed in neuronal and some glial populations in the rat brain. The localization of CYP2D1 in several regions known to harbor catecholamines and serotonin may suggest a role for CYP2D1 in the metabolism of monoamines.

Indexing terms: neurotoxin, Parkinson's disease, catecholamine metabolism, polymorphism, xenobiotics

Cytochrome P450s play an important role in the oxidative metabolism of various endogenous and xenobiotic compounds. Cytochrome P450 isoforms display overlapping substrate specificities; this capacity allows these enzymes to metabolize and detoxify many substances in the diet and environment (Gonzalez, 1989). Sites of expression of human and rat P450 genes and proteins have been found in the liver, lung, steroidenogenic tissue (Guengerich, 1992), nasal epithelium (Hadley and Dahl, 1982; Nef et al., 1989), and the brain. Using immunohistochemical techniques, the isoforms CYP1A1, CYP1A2, CYP2B1, CYP2B2, and CYP2E1 have been demonstrated in the rat and/or human brain (Kapitulnik et al., 1987; Köhler et al., 1988; Warner et al., 1988; Hansson et al., 1990). Other studies have demonstrated the activity of several P450 isoforms in microsomal or mitochondrial brain fractions (Ravindranath et al., 1989; Anandatheerthavarada et al., 1990; Iscan et al., 1990; Tyndale et al., 1991; Bhamre et al., 1993; Ghersi-Egea et al., 1993). The polymerase chain reaction technique has also revealed cytochrome P450 expression in the brain of rats, some of which were treated with compounds known to induce hepatic cytochrome P450 enzymes (Hodgson et al., 1993). The enzyme NADPH cytochrome P450 oxidoreductase is a major component of the mixed function oxidase system where it transfers electrons from NADPH to the different forms of cytochrome P450. NADPH cytochrome P450 oxidoreductase has a widespread distribution in the rat brain (Haglund et al., 1984; Norris et al., 1994).

Many of the genes encoding P450 enzymes show genetic polymorphisms, some of which produce functionally abnormal or inactive enzymes (Guengerich, 1992). Polymorphisms of *CYP2D1* (the designation for the enzyme is

Accepted May 12, 1995.

Address reprint requests to Dr. P.J. Norris, MRC Molecular Neuroscience Group, Department of Neurobiology, The Babraham Institute, Babraham, Cambridge, CB2 4AT, U.K.

CYP2D1 for rat and canine and CYP2D6 in humans, and *CYP2D1* and *CYP2D6* respectively for the corresponding genes, Nebert et al., 1991) have been associated with impaired oxidation of many drugs with diverse pharmacological actions, including the antiarrhthymic agent sparteine, the adrenergic blocking agent debrisoquine and the B-adrenoceptor antagonist bufuralol (Skoda et al., 1988; Lledó, 1993).

Polymorphisms of *CYP2D6* have been suggested to be associated with susceptibility to Parkinson's disease over many years (Barbeau 1985; Ferrari et al., 1986), and two recent papers have correlated the frequency of mutant *CYP2D6* alleles associated with poor metabolism of debrisoquine and an increased incidence of Parkinson's disease (Armstrong et al., 1992; Smith et al., 1992). Antibodies to the rat CYP2D1 enzyme have been shown to recognize the human enzyme and have been used to isolate human *CYP2D6* cDNA (Gonzalez et al., 1988; Tyndale, et al., 1991). CYP2D1 and the dopamine transporter are both [^{3}H]GBR-12935 binding proteins. Niznik et al. (1990) purified the proteins from canine striatal membranes using wheat germ agglutinin-lectin column chromatography and revealed that CYP2D1 and the dopamine transporter share some substrate/inhibitor specificities, although they are neither immunologically related nor similar at the amino acid level. The transporter family has 12 putative transmembrane domains (Giros and Caron, 1993), whereas microsomal cytochrome P450s are thought to be bound to the endoplasmic reticulum by only one or two transmembrane peptides located toward the hydrophobic amino terminus (Black, 1992). The purpose of this paper is to determine the localization of CYP2D1 immunoreactivity and CYP2D mRNA expression at the regional and cellular level and to look for associations with the distribution of neurotransmitters.

MATERIALS AND METHODS

Immunohistochemistry

The antiserum was raised in rabbits to CYP2D1 protein purified from rat liver microsome preparations (Gonzalez et al., 1987). The specificity of this antiserum has been characterized extensively in previous reports (Gonzalez et al., 1987, 1988). Four male Wistar rats (150–200 g) were terminally anaesthetized with pentobarbital (60 mg/kg) and perfused transcardially (via the ascending aorta) with 100 ml of 0.1 M phosphate buffered saline, pH 7.4 (PBS), containing 1% heparin followed by 200 ml of fixative containing 4% paraformaldehyde (PFA) in 0.1 M phosphate buffer, pH 7.4 (PB). The brains were removed from the skull and postfixed for 4 hours at 4°C, in the same fixative, prior to transfer to 0.1 M PBS containing 30% (w/v) sucrose for 3 days at 4°C. Coronal or sagittal sections (30 μm) were cut on a freezing microtome and collected in wells containing 0.1M PBS. The sections were incubated free-floating in anti-CYP2D1 antiserum diluted 1:3,000 in PBS containing 0.5% Triton X-100 and 1% normal goat serum (Dako Patts, Copenhagen, Denmark) for 1–2 days at 4°C. The antigen-antibody complex was visualised using the avidin-biotin complex (ABC) method of Hsu et al. (1982), using the ABC kit (Vector Laboratories, Burlingame, CA) with 3′, 3′-diaminobenzidine (DAB; Sigma Chemical Co., St. Louis, MO) as the chromogen. Sections were then rinsed in distilled water, air dried and delipidated in xylene and then coverslipped with Ralmount (Formulation by R. A. Lamb; BDH). In control experiments tissue was processed in tandem, but was incubated instead with anti-CYP2D1 Immunoglobulin G preabsorbed with the pure antigen. For preabsorbtion 100 μg of pure antigen was incubated with 1 ml of diluted antibody for 24 hours at 4°C.

In situ hybridization

For the detection of CYP2D-specific mRNA, two antisense oligodeoxynucleotide sequences (2 × 33 mers) which correspond to the bases 897–929 and 1316–1348 of the rat CYP2D1 mRNA (Genbank accession no M166654, ID code RNCYPDB1) were synthesized and then radiolabeled with ^{35}S-dATP (New England Nuclear, Boston, MA) using terminal deoxynucleotidyl transferase (Pharmacia, Piscataway, NJ). The radiolabeled probes were purified by gel filtration on Sephadex G-50. Two probes were mixed and

Abbreviations

ACB	nucleus accumbens
AO	anterior olfactory nucleus
APN	anterior pretectal nucleus
CB	cerebellum
CP	caudate putamen
CX	cerebral cortex
DG	dentate gyrus
DMH	dorsomedial nucleus hypothalamus
DR	dorsal nucleus raphé
GP	globus pallidus
HI,Hi	Hippocampus
IC	inferior colliculus
INT	interposed cerebellar nuclei
IPN	interpeduncular nucleus
Isl	islands of Calleja
LC	locus coerulcus
LD	lateral dorsal nucleus thalamus
MD	mediodorsal nucleus thalamus
MGv	medial geniculate complex, ventral part
MH	medial habenula
MM	medial mammilliary nucleus
MT	medial terminal nucleus of the accessory olfactory tract
ND	nucleus of Darkschewitsch
NI	nucleus incertus
NPC	nucleus of the posterior commissure
NTB	nucleus of the trapezoid body
OB	olfactory bulb
OT	olfactory tubercle
PAG	periaquaductal gray
PCG	pontine central gray
PG	pontine gray
PiG	pineal gland
PIS	pineal stalk
PSV	principal sensory nucleus of the trigeminal
PVH	paraventricular nucleus hypothalamus
RE	nucleus reuniens
RH	rhomboid nucleus
RN	red nucleus
SC	superior colliculus
SCi	superior colliculus intermediate gray layer
SN	substantia nigra
SO	supraoptic nucleus
STN	subthalamic nucleus
TT	taenia tecta
V	motor nucleus of the trigeminal nerve
VAL	ventral anterior-lateral complex thalamus
Ve	vestibular nucleus
VMH	ventromedial nucleus hypothalamus
VP	ventral posterior nucleus thalamus

used together to increase the specific activity of the bound probe.

Four male Wistar rats (150–200 g) were briefly anaesthetised with CO_2 and then killed immediately by decapitation. The brains were removed and frozen quickly on dry ice. Frozen sections (15 μm) were cut using a cryostat (Brights, Huntingdon, U.K.) and thaw mounted on gelatin/chrome-alum-coated glass slides. These slides were kept at −70°C until used. In situ hybridization was performed as described earlier with some slight modifications (Kadowaki et al., 1994; Norris et al., 1994). Frozen sections were fixed with 4% PFA in 0.1 M PB for 30 minutes at room temperature, rinsed twice with 0.1 M PBS pretreated with 0.1% diethylpyrocarbonate (DEPC). Sections were dehydrated through 70%, 80%, 90%, and 95% ethanol to absolute ethanol (5 minutes each) and then air dried. Dried sections were hybridized for 17 hours at 37°C in the following buffer: 4× standard saline citrate (SSC), 50% formamide, 1× Denhardt's solution, 500 μg/ml sheared salmon sperm DNA, 0.25 mM dithiothreitol (DTT), and 10% dextran sulphate. The ^{35}S-labeled probes were used at a concentration of approximately 4 fmol/μl. Hybridized sections were dipped in 1× SSC/0.001% B-mercaptoethanol to remove the hybridization buffer, washed stringently 4 times in 1× SSC /0.001% B-mercaptoethanol pre-heated to 55°C for 30 minutes each and washed again in 1× SSC /0.001% B-mercaptoethanol for 1 hour at room temperature. Sections were then rinsed briefly in distilled water, followed by 70% ethanol/300 mM ammonium acetate and finally rinsed briefly in absolute ethanol and air dried before exposing to film (Hyperfilm, B-max) for autoradiography. The sections were then processed by emulsion autoradiography. Ilford K-5 nuclear track emulsion was used and the slides were exposed for 6–9 weeks in a tight dark box. Sections were developed with D-19 (Kodak) for 2.5 minutes at 20°C, fixed with Ilfohypam (Ilford, U.K.) for 10 minutes and washed with tap water for 15 minutes. Slides were coverslipped in a 10 mM Tris-HCl (pH 7.5), 10 mM EDTA, and 50% glycerol solution.

Northern blot analysis

Poly $(A)^+$ mRNA was purified from whole rat brain using a micro fast track mRNA isolation kit (Invitrogen), and total RNA was purified from rat liver using the acid guanidinium thiocyanate-phenol-chloroform extraction procedure of Chomczyski and Sacchi (1987). RNA concentrations and purity were determined using a spectrophotometer (Howe & Co. Ltd. Oxon, UK). Rat brain poly $(A)^+$ RNA (3 μg per well) and rat liver total RNA (15 μg per well) were size-separated electrophoretically under denaturing conditions in a 1.5% agarose/0.66 M formaldehyde/1× morpholinopropane sulphonic acid gel containing ethidium bromide (3 mg/ml) and capilliary blotted onto Hybond-N membrane (Amersham) with 20× SSC. RNA was cross-linked to the membrane by UV irradiation (4 minutes). For the detection of CYP2D-specific mRNA the two oligodeoxynucleotides used for in situ hybridization were radiolabeled with (^{32}P)-dATP using terminal deoxynucleotidyl transferase to specific activity of 1×10^6 dpm/μg. The radiolabeled probes were purified by gel filtration on Sephadex G-50. The membrane was incubated in a prehybridization buffer (4× SSC/50% deionized formamide, 1× Denhardt's solution/500 μg/ml sonicated salmon sperm DNA/0.1% sodium dodecyl sulphate (SDS)/10% dextran sulphate) for 5 hours at 40°C, the probes were added and hybridized for 16 hours at 40°C washed in 1× SSC, 0.1% SDS (15 minutes at 38°C, 30 minutes at 50°C) followed by a brief wash in 1× SSC at room temperature, wrapped in Saran Wrap (Dow), and exposed to autoradiography film (Hyperfilm-B max; Amersham) with intensifying screens at -70°C for 4 days.

TABLE 1. Summary of the Levels of CYP2D1-like Immunoreactivity and CYP2D-Specific mRNA Expression in Some of the Brain Regions Examined[1]

Brain area	Immunoreactivity	mRNA expression
Olfactory bulb	+++	++
Olfactory tubercle	+++	+/++
Nucleus accumbens	+/++	+/++
Piriform cortex	++	+++
Cerebral cortex	+++	++
Caudate putamen	++/+++	+/++
Globus pallidus	+/++	+/++
Hippocampus (pyramidal cell layer)	++/+++	+++
Dentate gyrus (granule cell layer)	++	+++
Supraoptic nucleus	+++	+++
Medial habenula	+++	++/+++
Hypothalamus	++	++/+++
Thalamus	++	++
Mammilliary nuclei	+++	+++
Substantia nigra	++/+++	+/++
Red nucleus	+++	++
Locus coeruleus	+++	++
Cerebellum (granular cell layer)	+	++/+++
Cerebellum (Purkinje cell layer)	+++	+++
Cerebellum (Bergmann glia)	++/+++	++/+++

[1]The intensity of the immunostaining and mRNA expression was scored by eye as follows: +, weak; ++, moderate; +++, strong.

RESULTS

The stereotactic atlas of Swanson (1992) was used to identify nuclei and regions within coronal sections of rat brain. The levels of CYP2D1 like immunoreactivity and CYP2D mRNA signal in 20 regions of the rat brain are summarized in Table 1.

Distribution of CYP2D1 immunoreactivity in the rat central nervous system

The purification and specificity of the anti-rat CYP2D1 antibody used in this study has been extensively documented in previous reports (Gonzalez et al., 1987, 1988). In control experiments, free-floating rat brain sections were not stained in the absence of primary antiserum and incubation of brain sections in anti-CYP2D1 Immunoglobulin G preabsorbed with the pure antigen (100 μg per 1,000 μl diluted antibody at 4°C for 24 hours) blocked staining in all of the brain regions examined (Fig. 1).

Telencephalon In the olfactory bulb, immunohistochemistry revealed staining of neurones in the granular and mitral cell layers. In the outer plexiform layers, there was staining of glia and the neuropil, increased staining in or around the glomeruli and intense staining of fibre tracts surrounding the main olfactory bulb, and particularly strong immunoreactive staining of the anterior olfactory nucleus (Fig. 1A, Table 1). In the olfactory tubercle, glial cells were stained predominantly in layers 1 and 2, and there was some light staining of neuronal cell bodies in layer 3 (Table 1).

The islands of Calleja, a population of large neurones in the substantia inominata, and neurons in the nucleus accumbens were also lightly stained (Table 1). Moderate immunostaining of pyramidal cells was detected in layer 2 of the piriform cortex (Table 1). In the neocortex, high levels of immunoreactivity were observed in layers I, II, III, and V (Table 1). Immunohistochemistry revealed staining

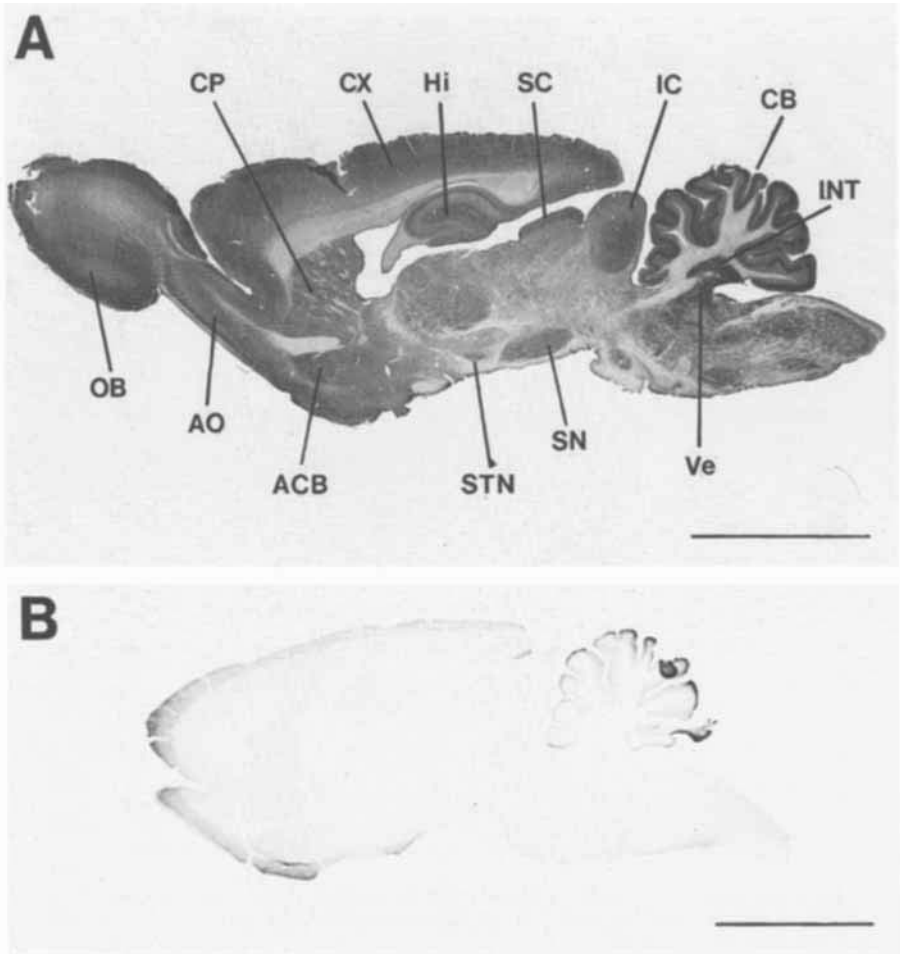

Fig. 1. Photomicrographs showing sagittal sections through the rat brain incubated with anti-CYP2D1 immunoglobulin G **(A)**, or incubated with anti-CYP2D1 immunoglobulin G preabsorbed with the pure antigen **(B)**. Scale bars = 5 mm. See abbreviations list for details.

of glial cells and neuropil in layer I, in layers II and III there was strong staining of large numbers of densely packed cells, presumably stellate and pyramidal cells (Fig. 2A). Pyramidal cells in all layers except layer VI were strongly immunoreactive; in layers IV and V the cytoplasmic staining of the apical dendrites of these cells could be clearly visualized (Fig. 2B). In the caudate putamen there was immunoreactive staining of the neuropil and staining of a population of cell bodies ranging from 14 to 28 μm in diameter (Fig. 3A, Table 1). In the globus pallidus a similar pattern of neuropil staining was observed, and there was positive staining of a population of neurons approximately 24 μm in diameter (Fig. 3A, Table 1).

In all subfields (CA1–3) of the hippocampus there was moderate staining of pyramidal cell bodies and their processes extending in to the stratum radiatum (Fig. 4 A,B, Table 1). Additionally, there was a population of large, intensely stained cell bodies which were predominantly in the stratum pyramidal and stratum oriens, but also found in the stratum radiatum and stratum lacunosum-moleculare (Fig. 4A,C). In the dentate gyrus there was moderate staining of granule cells (Table 1) and staining of a population of neurones and glial cells in the polymorph layer (Fig. 4E). In the molecular layer of the medial blade of the dentate gyrus strongly immunoreactive glial cells were observed (Fig. 4D).

Diencephalon There were populations of intensely positive neurones in the supraoptic nucleus and medial habenula (Fig. 5A,B, Table 1). High levels of immunoreactivity were also observed in the choroid plexus, lateral, medial and ventral hypothalamic area (Table 1), and the median eminence (Fig. 6A). Immunoreactive neurones were detected in essentially all the thalamic nuclei, the strongest labeling was found in the ventral and lateral posterior thalamic nucleii (Table 1). In the subthalamic nucleus there was moderate staining of cell bodies and the surrounding neuropil (Fig. 1A).

Mesencephalon Moderately immunoreactive cell bodies were also evident in the lateral and medial geniculate complex (dorsal and ventral parts) (Fig. 6B). Immunoreactive cell bodies were evident in the periaquaductal grey and nucleus of the posterior commissure and there was strong labeling of the habenular commissure and subcommissural organ (Fig. 6C). The cell bodies and neuropil of the medial and lateral mamilliary nuclei were immunoreactive (Table 1) as were the cell bodies in the lateral and medial parts of the supramammilliary nucleus, ventral and dorsal parts of

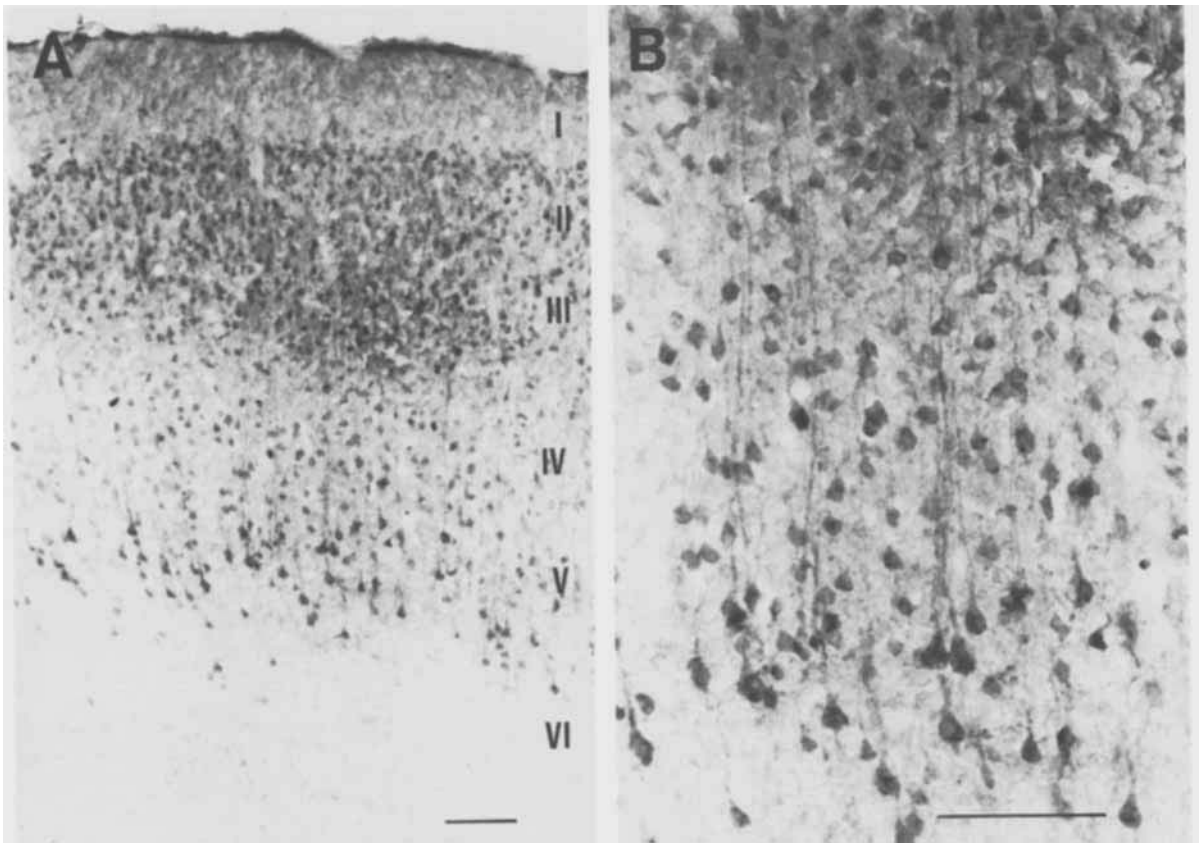

Fig. 2. Photomicrographs of coronal sections through the cerebral cortex. **A:** Pyramidal cells in layers II, III and V were strongly immunoreactive. **B:** Enlargement of pyramidal cells in A showing staining of apical dendrites. Scale bars = 100 μm.

the premammilliary nucleus and the posterior periventricular region surrounding the third ventricle (Fig. 6D)

In the substantia nigra pars compacta the cell bodies were darkly stained, and in the pars reticulata cell bodies and their processes were strongly immunoreactive (Table 1) as were cell bodies in the medial terminal nucleus of the accessory optic tract and the ventral tegmental area (Fig. 3B). In the cerebral peduncle there was heavy staining of fibres and glia. There was moderate immunoreactivity in the interpeduncular nucleus and strong staining of the pontine grey. In the superior colliculus the neurones in the superficial grey layer and the zonal layer were moderately immunoreactive and the inferior colliculus was also moderately stained (Fig. 1A). A population of large neurones and their processes were immunoreactive in the red nucleus (Fig. 7C, Table 1) and there was heavy staining of neurones of the nucleus of Darkschewitsch and the oculomotor nucleus.

Pons and medulla Darkly stained cell bodies were observed in the pontine central grey; locus coeruleus (Table 1); nucleus incertus (Fig. 7A); nucleus of the trapezoid body; mesencephalic nucleus, large neurones and neuropil of the lateral, medial, and superior spinal vestibular nucleus; and also some glial staining in the pyramidal tract (Fig. 1A). Cell bodies associated with the interposed cerebellar nucleus (anterior and posterior) and the nuclei of the trigeminal nerve were also strongly immunoreactive.

In the cerebellum there was strong staining of the Purkinje cells (Table 1). The granular cell layer was lightly stained; some of the staining appeared to be glial. In the molecular layer there was intense staining of Bergmann glia and processes (Fig. 7B, Table 1).

Spinal cord In the spinal cord there was CYP2D1-like immunoreactivity in the gray matter of the dorsal and ventral horns, strong staining of motor neurones, and staining of glial cells in the surrounding white matter (Fig. 7D).

Distribution of CYP2D-specific mRNA expression in the rat central nervous system

The two antisense oligonucleotides were prepared to CYP2D-specific sequence data. One probe shared greater than 84% homology, and the second probe shared 100% homology with all five sequenced members of the rat CYP2D gene family. In order to ascertain the specificity of the probes for in situ hybridization analysis poly $(A)^+$ RNA from whole rat brain and rat liver was probed with the ^{32}P-labeled antisense oligonucleotide probes. In the poly $(A)^+$ RNA blots the probes hybridized to one rat liver mRNA species approximately 1.7 kb in size and two rat brain mRNA species which were approximately 2.0 and 2.9 kb (Fig. 8). In in situ hybridization experiments the specificity of the CYP2D signal was confirmed by the use

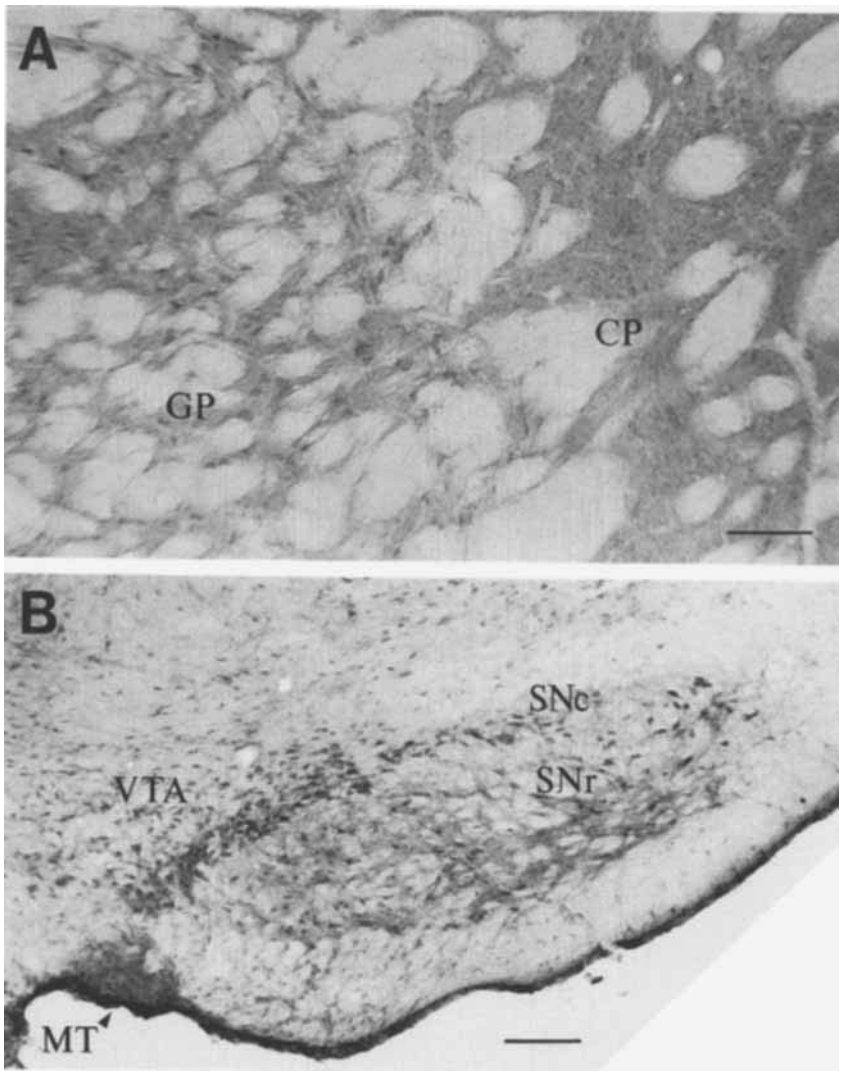

Fig. 3. **A:** Photomicrograph of the distribution of CYP2D1 immunoreactivity in the caudate putamen and globus pallidus showing staining of the neuropil and cell bodies. Scale bar = 100 μm. **B:** Photomicrograph of a coronal section through the substantia nigra showing strong staining of neurones in the pars compacta (SNc) and strong staining of neurones and neuropil in the pars reticulata (SNr), ventral tegmental area (VTA), and medial terminal nucleus of the accessory olfactory tract (MT). Scale bar = 200 μm.

of 100-fold molar excess of unlabeled oligonucleotides which completely displaced specific binding (Figs. 9D, 10H). As expected there was intense labeling of rat liver sections by the two CYP2D-specific oligonucleotide probes (Fig. 9C).

Telencephalon In the main olfactory bulb CYP2D mRNA expression was strongest in the granular and mitral cell layers, with lower levels of expression in the outer plexiform layers and surrounding the glomeruli (Fig. 9A, Table 1).

Low to moderate levels of mRNA expression were detected in the olfactory tubercle (Table 1), and the islands of Calleja (Fig. 10A, Fig. 11A). There was weak mRNA signal in the nucleus accumbens (Table 1) and moderate levels in the dorsal part of the taenia tecta (Fig. 10A).

There was particularly strong mRNA expression of the pyramidal cells in layer 2 of the piriform cortex (Figs. 10A, 11B; Table 1). In the neocortex moderate levels of mRNA signal were observed in layers I, II, III, and V (Fig. 10A–D, Table 1). There were weak to moderate levels of mRNA expression over cell bodies in the caudate putamen and globus pallidus.(Fig. 10A,B, Table 1).

High levels of mRNA signal were detected in cells of the pyramidal layer in all subfields of the hippocampus and in the medial blade polymorph layer and medial and lateral blade granule cell layers (Fig. 10B–D, Table 1).

Diencephalon There were populations of neurones expressing high levels of mRNA in the supraoptic nucleus and medial habenula (Figs. 10B,C, 11C,D, Table 1). High levels of mRNA expression were also observed in the choroid plexus, lateral, medial and ventral hypothalamic area and the arcuate nucleus hypothalamus and paraventricular nucleus hypothalamus (Fig. 10B,C, Table 1). Moderate mRNA signal was detected in most regions of the thalamus (Table 1), the strongest mRNA signal was found in the venteral/lateral posterior thalamic nuclei (Fig. 10B,C).

Mesencephalon Medium to high levels of mRNA expression were detected in cell bodies in the lateral and medial

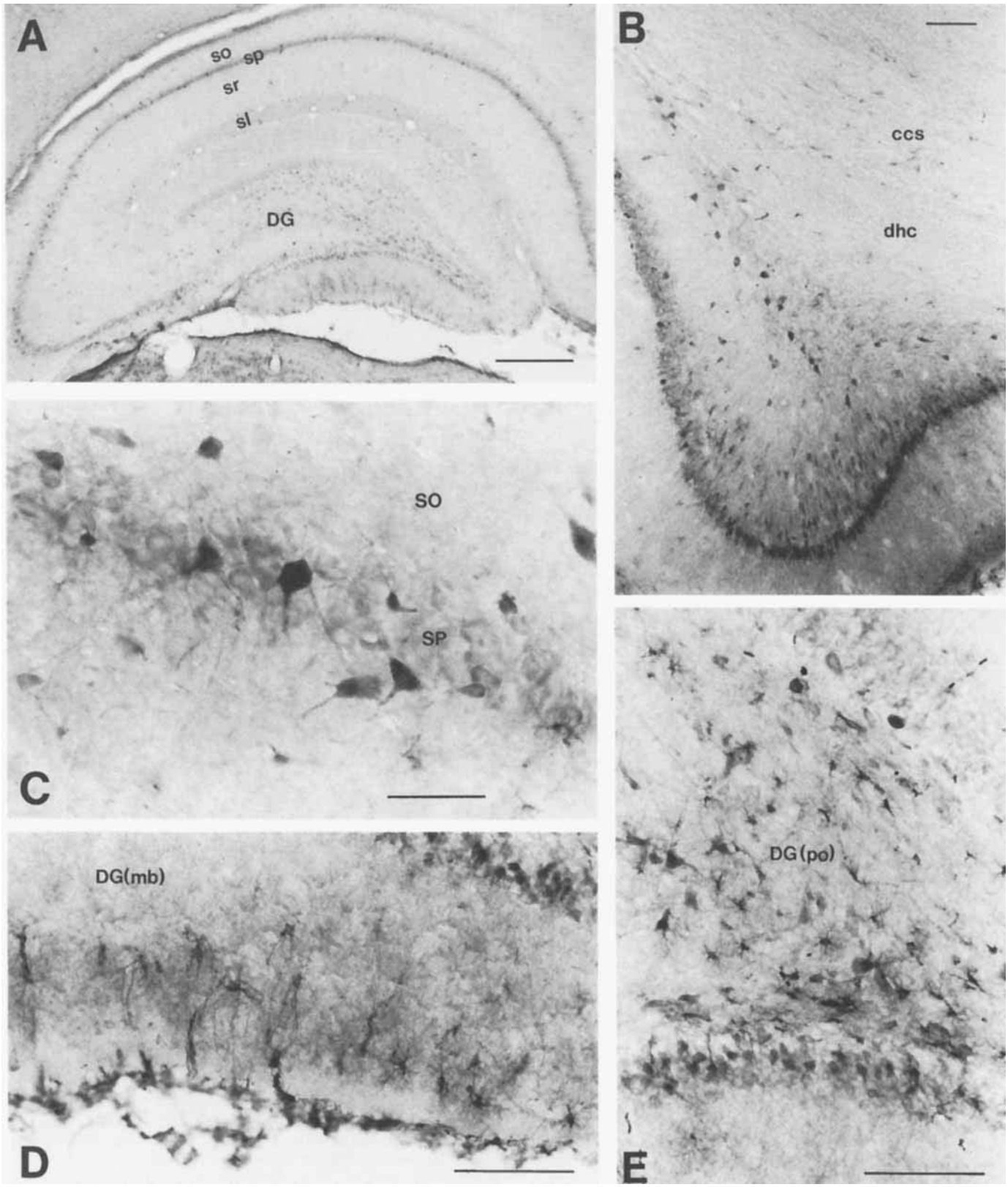

Fig. 4. Photomicrographs showing cytochrome CYP2D1 immunoreactivity in the hippocampus and the dentate gyrus. **A:** Coronal section through the hippocampus showing the distribution of CYP2D1 immunoreactivity in the stratum oriens (so), stratum pyramidal (sp), stratum radiatum (sr) and stratum lacunosum-moleculare (sl) and in the dentate gyrus. Scale bar = 500 μm. **B:** Staining of cells in the pyramidal cell layer beneath the dorsal hippocampal commissure (dhc) and corpus callosum splenium (ccs). Scale bar = 100 μm. **C:** Staining of neurones in the stratum oriens (SO) and stratum pyramidal (SP) in the CA2 subfield of the hippocampus. Scale bar = 50 μm. **D:** Staining of glial cells in the medial blade of the dentate gyrus (DG(mb)). Scale bar = 100 μm. **E:** Staining of neurones and glial cells in the polymorph layer of the dentate gyrus (DG(po)). Scale bar = 100 μm.

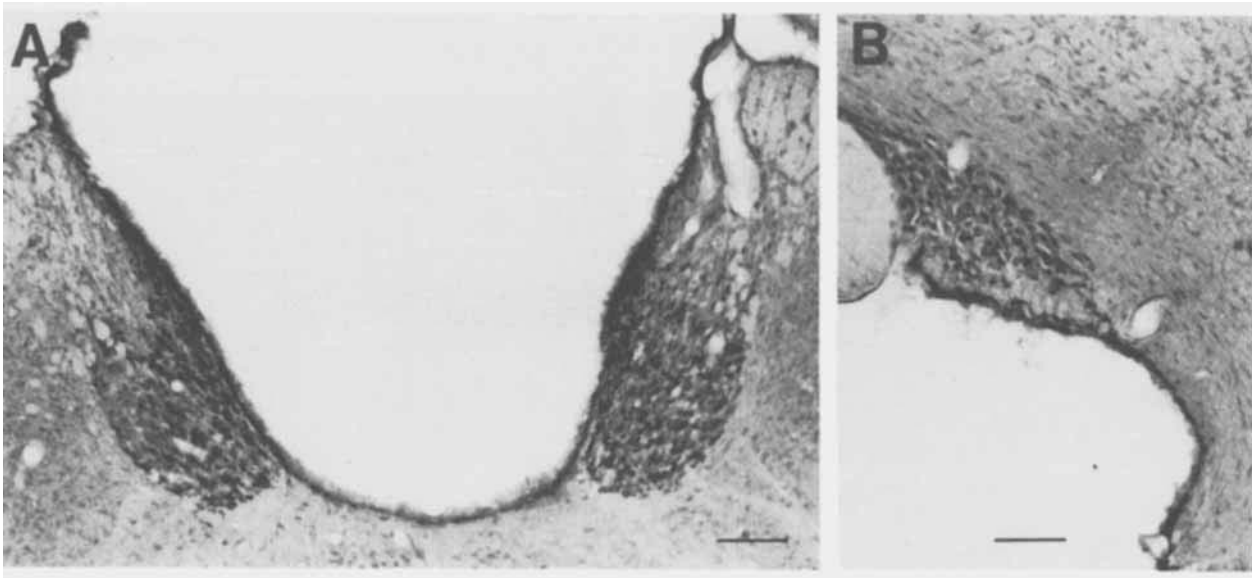

Fig. 5. Photomicrographs of coronal sections showing strong staining of the medial habenula **(A)** and the supraoptic nucleus **(B)**. Scale bars = 100 μm.

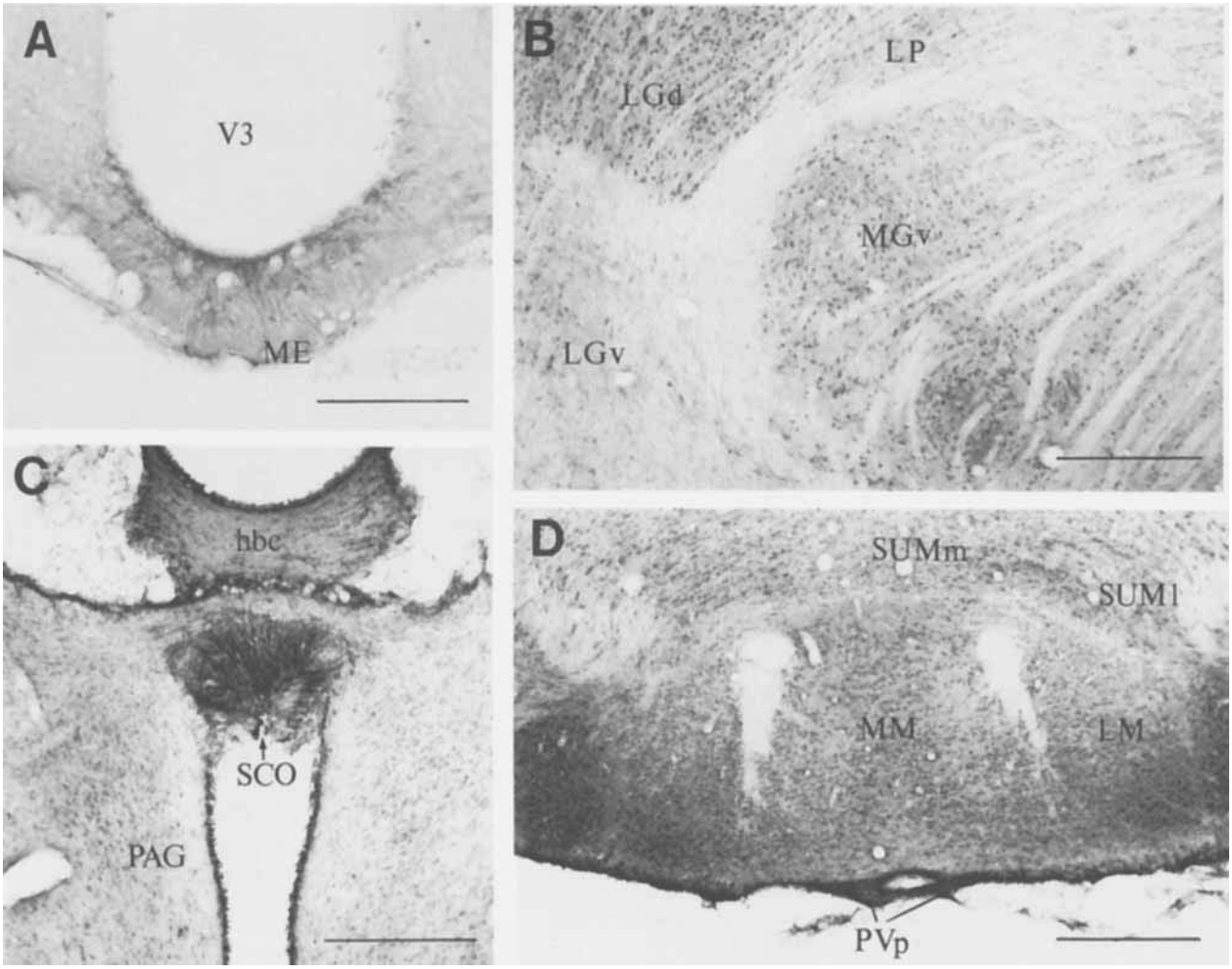

Fig. 6. Photomicrographs showing CYP2D1-immunoreactive cells. **A:** Coronal section through the third ventricle (V3) showing strong immunoreactivity in the median eminence (ME). Scale bar = 100 μm. **B:** Coronal section showing immunoreactive cell bodies and neuropil in the lateral postrior nucleus thalamus (LP), lateral geniculate complex, dorsal and ventral parts (LGd, LGv) and medial geniculate complex, ventral part (MGv). Scale bar = 200 μm. **C:** Coronal section showing strong immunoreactivity in the habenular commissure (hbc), and subcommissural organ (SCO) and strongly stained cell bodies in the periaqueductal gray (PAG). Scale bar = 200 μm. **D:** Coronal section showing strong immunoreactivity in the medial and lateral mammilliary nucleii (MM, LM); supramamilliary nucleus, medial and lateral parts (SUMm, SUMl); and the posterior periventricular nucleus hypothalamus (PVp). Scale bar = 200 μm.

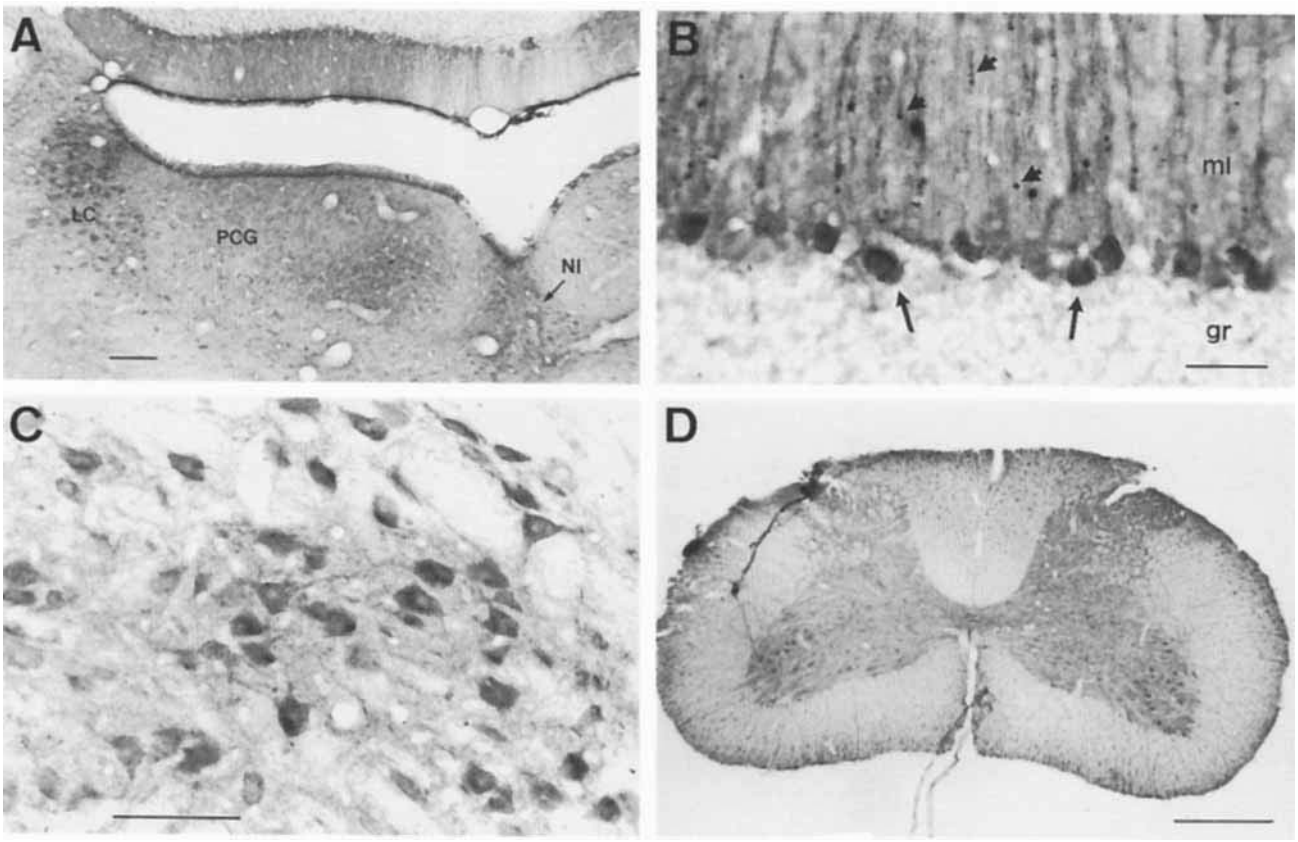

Fig. 7. Photomicrographs showing CYP2D1-immunoreactive cells. **A:** Coronal section showing staining of the pontine central gray (PCG), locus coeruleus (LC), and nucleus incertus (NI). Scale bar = 100 μm. **B:** Coronal section through the cerebellum showing light staining of the granular layer (gr); strong staining of Purkinje cells, indicated by black arrows, in the Purkinje layer; and strong staining of Bergmann glial cells and their processes, indicated by black arrowheads, in the molecular layer (ml). Scale bar = 50 μm. **C:** Strongly stained neurones and their processes in a coronal section through the red nucleus, scale bar = 100 μm. **D:** Staining of the dorsal and ventral horns, motor neurons, and white matter glial cells in the spinal cord. Scale bar = 500μm.

parts of the supramammilliary nucleus and ventral and dorsal parts of the premammillary nucleus (Fig. 10D, Table 1). A moderate in situ signal was also evident in the lateral and medial geniculate complex (dorsal and ventral parts), red nucleus (Table 1), nucleus of Darkschewitsch (Fig. 10D), superior colliculus and ventral tegmental area (Fig. 10E). In situ hybridization revealed moderately strong labeling in the substantia nigra pars compacta and a weaker signal in the pars reticulata (Fig. 10E, Table 1). In addition there was a strong signal in the interpeduncular nucleus (Fig. 10E), pontine grey, and pineal gland (Fig. 10F).

Pons and medulla Moderate mRNA signals were detected in the locus coeruleus (Table 1), nucleus of the trapezoid body, motor nucleus of the trigeminal nerve, principal sensory nucleus of the trigeminal, and superior olivary complex; and a weak signal was detected in the pontine central gray (Fig. 10G). In the cerebellum there was an intense mRNA signal over the Purkinje cells and a moderately strong signal over the granular cell layer (Table 1). In the molecular layer high levels of mRNA expression were detected immediately adjacent to and surrounding the Purkinje cells, the pattern resembling labeling of Bergmann glial cells (Fig. 9B, 10G, Table 1).

Spinal cord In the spinal cord high levels of CYP2D mRNA were expressed in the gray matter of the ventral and

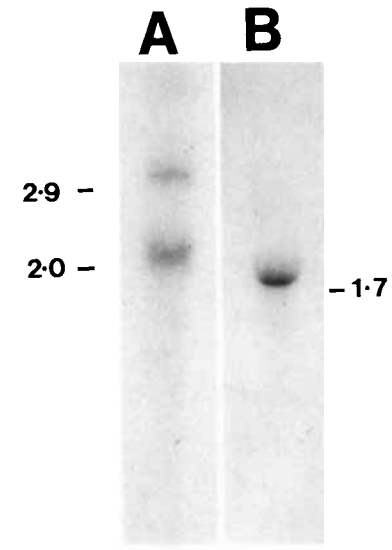

Fig. 8. Northern blot analysis of rat brain and rat liver CYP2D-specific mRNA expression. The sizes of the rat brain **(lane A)** and rat liver **(lane B)** mRNA species are indicated at the side of the blots.

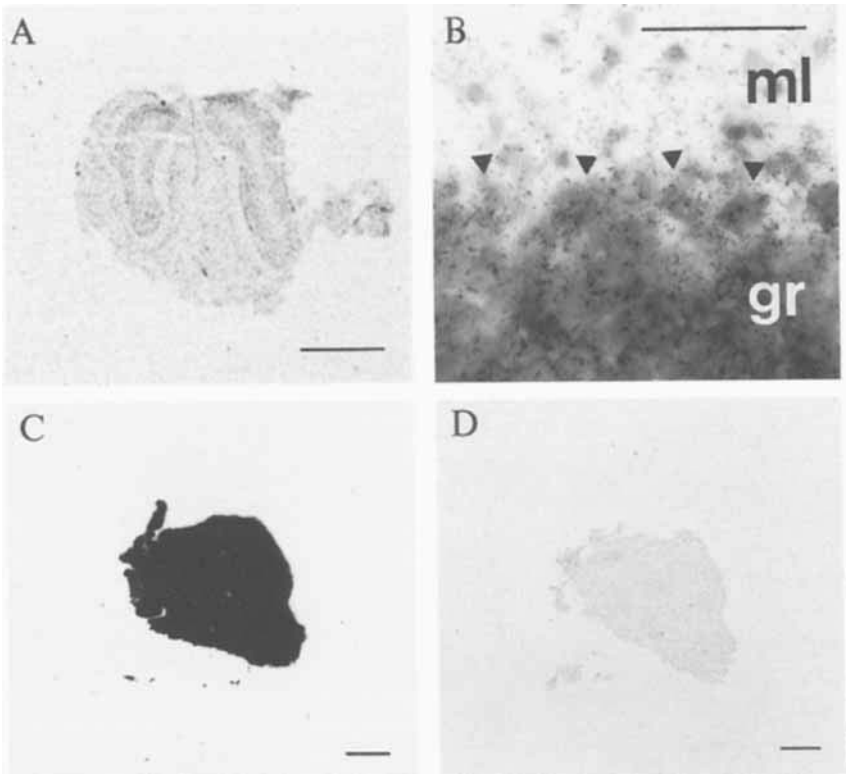

Fig. 9. Photomicrographs showing in situ hybridization using CYP2D-specific oligodeoxynucleotides probes. **A:** Coronal section through the rat olfactory bulb. Scale bar = 2 mm. **B:** Brightfield photomicrograph of a coronal section through the rat cerebellum showing the weak labeling of the molecular layer (ml), moderate labeling of the granule cell layer (gr), and strong labeling of the Purkinje cell layer (indicated by black arrowheads). Scale bar = 60 μm. **C:** Strong labeling of rat liver. Scale bar = 2 mm. **D:** Strong labeling of rat liver is displaced by an excess of unlabeled oligonucleotides. Scale bar = 2 mm.

dorsal horns, there was particularly strong labeling of motor neurones.

DISCUSSION

The present study describes the regional and cellular localization of CYP2D1-like immunoreactivity and CYP2D mRNA expression in the rat central nervous system. The distribution of CYP2D1 protein was investigated using immunohistochemistry. CYP2D1-like immunoreactivity was found to be widespread in neuronal cells and present in some glial populations. Particularly strong CYP2D1-like immunoreactivity was seen in the olfactory bulb, olfactory tubercle, optic tract, piriform cortex, cerebral cortex, caudate putamen, hippocampus, medial habenula, supraoptic nucleus, substantia nigra, medial mamilliary nuclei, red nucleus, colliculi, several nuclei in the brainstem, and the cerebellum.

Northern blot analysis of rat brain poly(A)$^+$RNA using two CYP2D-specific oligodeoxynucleotide probes indicated the presence of two species of CYP2D mRNA. The major band was approximately 2.0 kb in size and the minor band was approximately 2.9 kb in size. This agrees with the findings of Komori (1993), who also detected two CYP2D mRNA-specific bands in rat brain. The rat CYP2D subfamily contains five members, 2D1 to 5 (Nelson et al., 1993); however, only *CYP2D4* and *CYP2D1* cDNA have been isolated from screened rat brain libraries, suggesting that these may be the only CYP2D isoforms that are expressed constitutively in the rat brain (Komori, 1993). CYP2D mRNA was expressed broadly in the rat brain. In many regions of the brain the signal was at relatively low abundance. High levels of expression were observed in specific brain regions; however, the degree of cellularity may be a contributing factor. Strong CYP2D mRNA expression was observed in the olfactory bulb, medial habenula, hippocampus, supraoptic nucleus, medial mamilliary nucleus, red nucleus, several regions of the brainstem, and the cerebellum. Particularly strong immunoreactivity usually corresponded with strong CYP2D mRNA signal and the overall distribution of CYP2D1-like immunoreactivity and CYP2D mRNA was very similar, suggesting CYP2D1 may be the main form of CYP2D expressed in rat brain.

In some regions the distribution of CYP2D1 immunoreactivity and CYP2D mRNA were dissimilar. Glial cells in the molecular layer of the medial blade of the dentate gyrus and a population of neurones in the stratum radiatum and stratum lacunosum-moleculare were strongly immunoreactive; however, there was no evidence of CYP2D mRNA expression by these cells. The absent or low mRNA signal may suggest that the strong immunoreactive signal by these cells may be due to the antibody binding to a CYP2D1-related antigen. In the granule cell layers of the cerebellum and dentate gyrus there was only weak immunoreactivity; however, in situ hybridization revealed strong

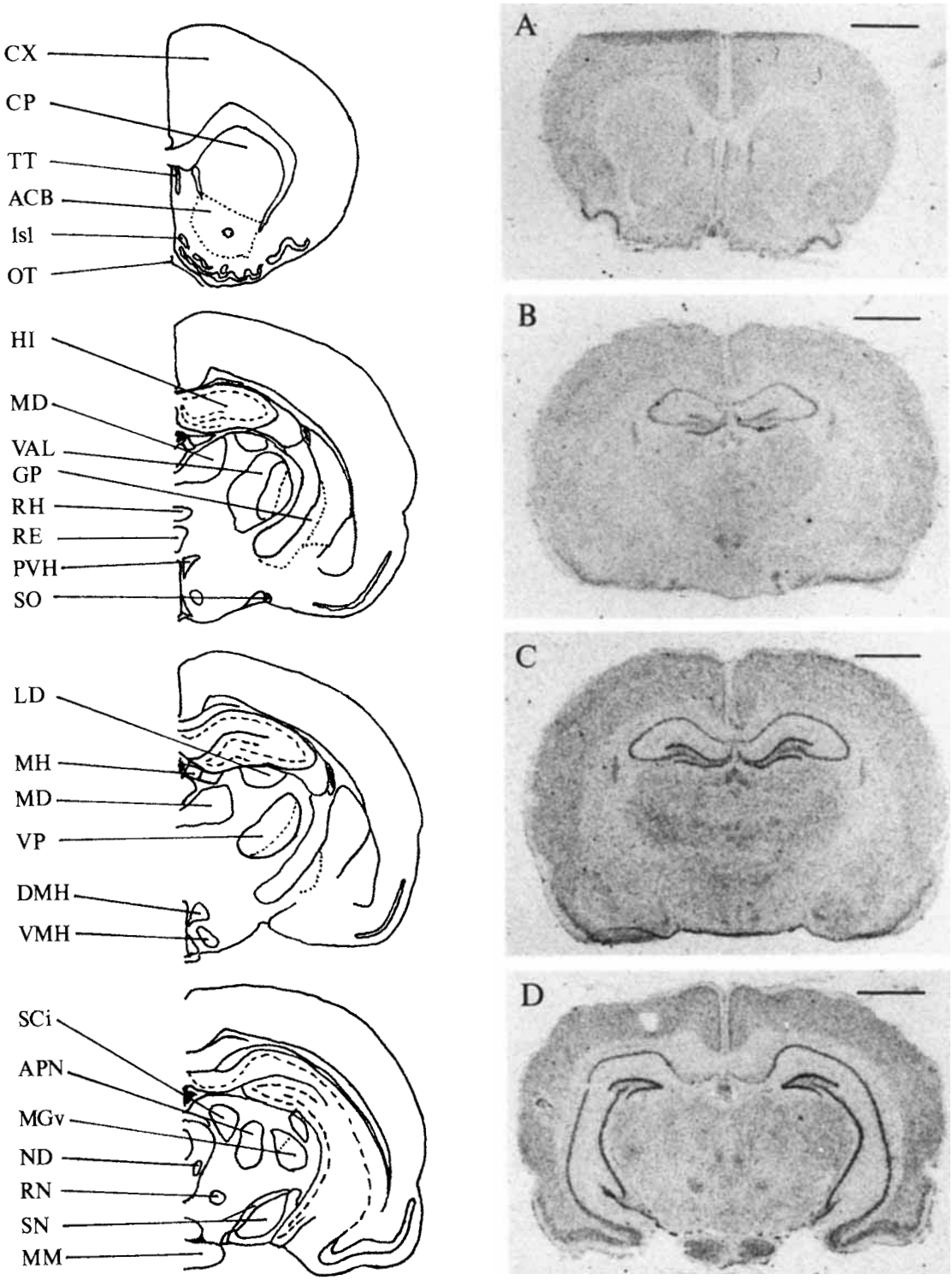

Fig. 10. Photomicrographs showing in situ hybridization of coronal rat brain sections **(A–H)** probed with ^{35}S-labeled CYP2D-specific oligodeoxynucleotides. Control section (H) cut at the same level as D where a 100-fold excess of unlabeled CYP2D oligodeoxynucleotides has displaced the specific binding seen in D. Scale bar = 2.5 mm. See abbreviations list for details.

CYP2D mRNA expression. This may perhaps be explained by reduced translation of the CYP2D1 mRNA, a high turnover of CYP2D1 protein in this area, or perhaps a rapid turnover of mRNA but not protein. Alternatively the oligonucleotides may be detecting another member of the CYP2D subfamily in this region.

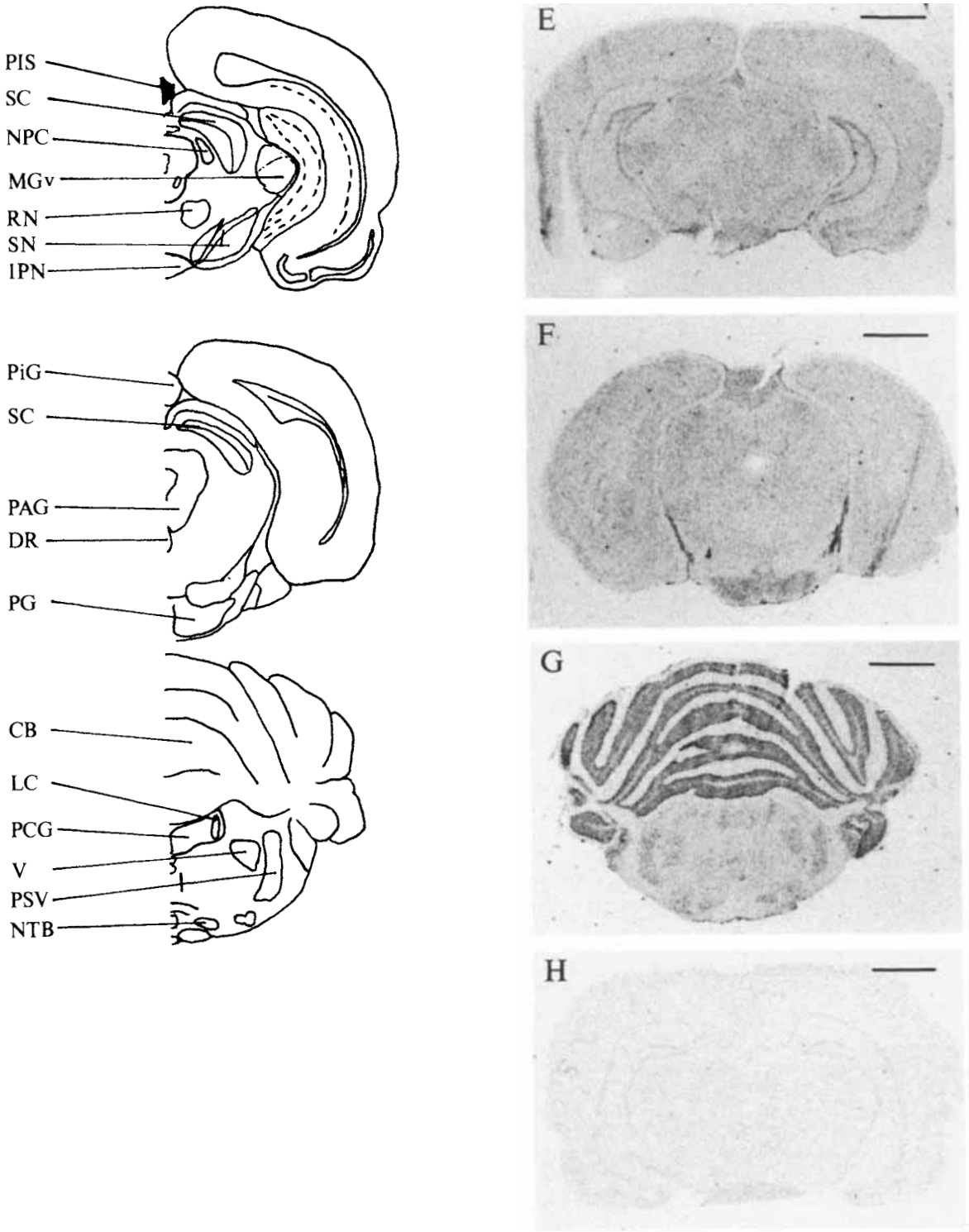

Figure 10 (Continued)

The overall pattern of distribution of CYP2D1-like immunoreactivity and CYP2D mRNA did not correspond with the distribution of any one distinct neurotransmitter system. However, the distribution of CYP2D1 did correspond with some regions known to contain the catecholamines dopamine and noradrenaline and the indoleamine serotonin. The widespread distribution of the enzyme CYP2D1 revealed in this study and the widespread distribution reported for the enzymes CYP2E1 (Hansson et al., 1990), CYP1A1, and CYP1A2 (Köhler et al., 1988; Warner et al.,

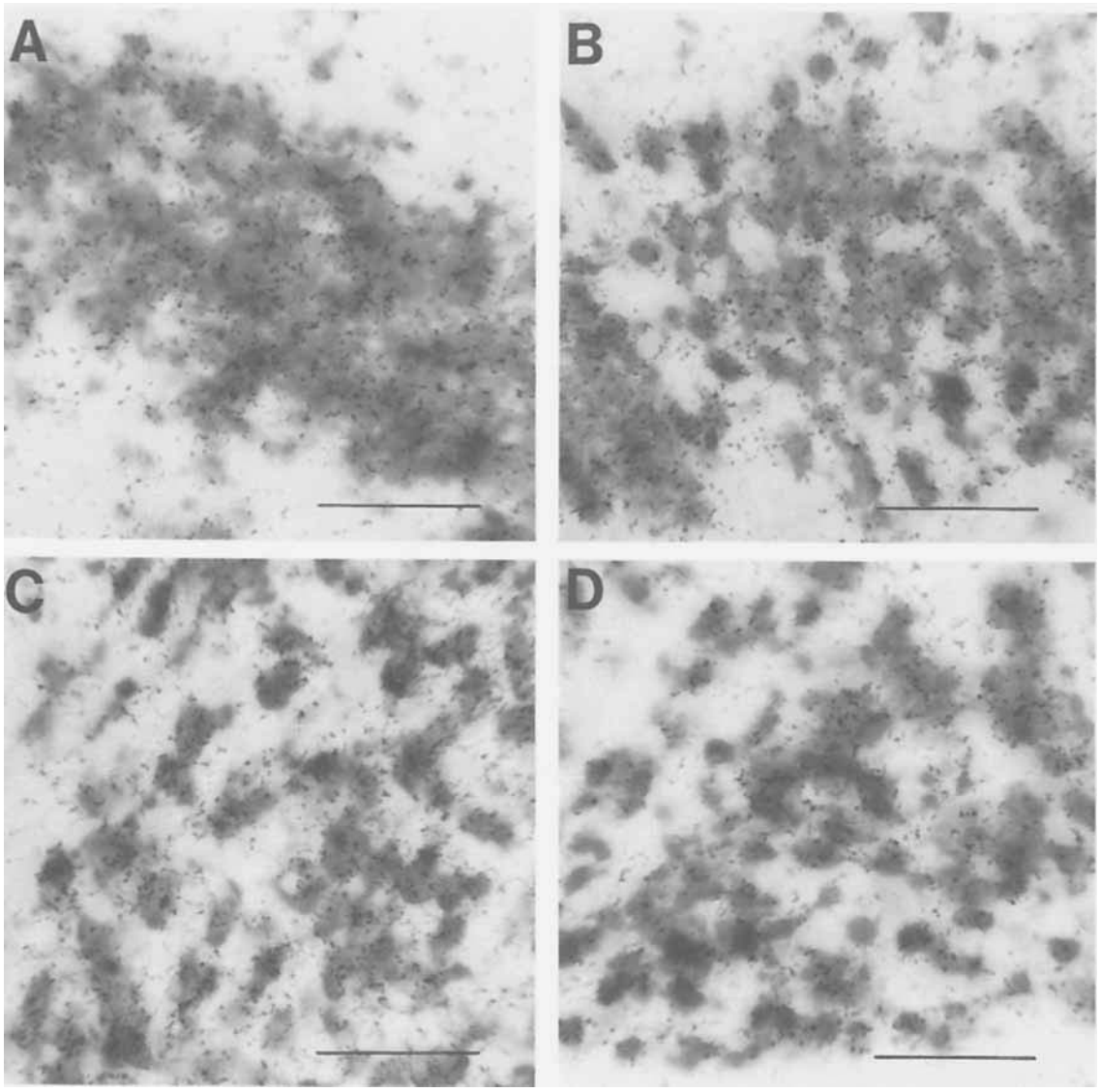

Fig. 11. Photomicrograph showing in situ hybridization using CYP2D-specific oligodeoxynucleotide probes. Groups of neurones expressing CYP2D mRNA in the islands of Calleja **(A)**, layer 2 of the piriform cortex **(B)**, supraoptic nucleus **(C)**, and medial habenula **(D)**. Probe binding is indicated by the presence of black silver grains in the overlying autoradiographic emulsion. Scale bars = 50 μm.

1988) suggests P450s may have an important role in brain metabolism. High levels of P450s have been reported in the rat nasal epithelium, a region with high exposure to xenobiotics, where it is likely that P450s may be important for the metabolism and detoxification of these compounds (Hadley and Dahl, 1982). Outside the nasal epithelium P450s maybe involved in similar actions degrading transmitters and other products of neuronal activity.

The presence of many [^{3}H]GBR-12935 binding sites has been demonstrated in the rat (Anderson, 1987) and human brain (Hirai et al., 1988; Marcusson and Eriksson, 1988). One of these binding sites has been identified as the dopamine transporter and the second has been termed the "piperazine acceptor" site (Anderson, 1987). In canine brain this piperazine acceptor site has been identified as CYP2D1 (Niznik et al., 1990). Allard et al. (1994) have described [^{3}H]GBR-12935 binding to the piperazine acceptor site in human. Their findings suggest at least part of the piperazine acceptor binding may be attributed to CYP2D6 and that this protein may be found in several regions of the human brain, including the cerebral cortex, hypothalamus, substantia nigra, caudate nucleus, putamen, and hippocampus.

The distribution of CYP2D6 is of particular interest as polymorphisms of this enzyme have been linked with an increased susceptibility to bladder and lung cancer (Gough et al., 1990) and also Parkinson's disease (Armstrong et al., 1992; Smith et al., 1992). Several studies have described the CYP2D6-mediated metabolism of 1-methyl-4-phenyl-1,2,3,6-tetrahydropyridine (MPTP), 1-methyl-4-phenylpyridine (MPP^+), and 1,2,3,4-tetrahydroquinoline (TIQ) in human and rat (Fonne-Pfister et al., 1987; Ohta et al., 1990; Shahi et al., 1989; Suzuki et al., 1992). These compounds are neurotoxic and have all been shown to induce Parkinson's

disease like symptoms. Budipine and proadifen, both of which inhibit CYP2D1 activity, have been reported to protect against MPTP and MPP+ induced neurotoxicity (Przuntek et al., 1985; Russ et al., 1986; Pai and Ravindranath, 1991).

Several monoamine oxygenase B substrates (e.g., MPTP, TIQ) and inhibitors (amiflamine, methoxyphenamine) are substrates of cytochrome CYP2D6. The enzyme monoamine oxygenase B is found on the outer membrane of mitochondria where it catalyses the deamination of noradrenaline and dopamine. Additionally tricylic antidepressants, cocaine, d-amphetamine, and related agents which inhibit the reuptake of dopamine via the dopamine transporter are also substrates of CYP2D6 (Tyndale et al., 1991; Cholerton et al., 1992). The distribution of CYP2D1 described here and the similarity between the substrate/inhibitor specificities of the dopamine transporter, monoamine oxygenase B and CYP2D1 (Niznik et al., 1990), point strongly towards one of the roles for CYP2D1 (CYP2D6 in humans) in the brain being the metabolism of monoamines in neurones. Given the linkage between CYP2D6 with Parkinson's disease, further investigation in this area may clarify the relationship between external and internal factors in the aetiology of Parkinson's disease.

ACKNOWLEDGMENTS

We are grateful for the continuing support of the Medical Research Council (UK). We thank Mr. I. King for emulsion autoradiography.

LITERATURE CITED

Allard, P., J.O. Marcusson, and S.B. Ross (1994) [^{3}H]GBR-12935 binding to Cytochrome P450 in the human brain. J. Neurochem. *62:*342–348.

Anandatheerthavarada, H.K., S.K. Shankar, and V. Ravindranath (1990) Rat brain cytochromes P-450: catalytic, immunochemical properties and inducibility of multiple forms. Brain Res. *536:*339–343.

Anderson, P.H. (1987) Biochemical and pharmacological characterization of [^{3}H] GBR-12935 binding *in vitro* to rat striatal membranes: labelling of the dopamine uptake complex. J. Neurochem. *48:*1887–1896.

Armstrong, M., A.K. Daly, S. Cholerton, D.N. Bateman, and J.R. Idle (1992) Mutant debrisoquine hydroxylation genes in Parkinson's disease. Lancet *339:*1017–1018.

Barbeau, A., M. Roy, S. Paris, T. Cloutier, L. Plasse, and J. Poirier (1985) Ecogenetics of Parkinson's disease: 4-hydroxylation of debrisoquine. Lancet *2:*1213–1216.

Bhamre, S., H.K. Anandatheerathavarada, S.K. Shankar, M.R. Boyd, and V. Ravindranath (1993) Purification of multiple forms of cytochrome P450 from a human brain and reconstitution of catalytic activities. Arch. Biochem. Biophys. *301:*251–255.

Black, S.D. (1992) Membrane topology of the mammalian P450 cytochromes. FASEB J. *6:*680–681.

Cholerton, S., A.K. Daly, and J.R. Idle (1992) The role of individual human cytochromes P450 in drug metabolism and clinical response. Trends Pharmacol. Sci. *13:*434–439.

Chomczyski, P., and N. Sacchi (1987) Single-step method of RNA isolation by acid guanidinium thiocyanate-phenol-chloroform extraction. Anal. Biochem. *162:*156–159.

Ferrari, M.D., F.A. DeWolff, P. Vermey, H. Veenema, and O.J.S. Buruma (1986) Hepatic cytochrome-P450 malfunction and Parkinson's disease. Lancet *1:*324.

Fonne-Pfister, R., M.J. Bargetzi, and U.A. Meyer (1987) MPTP, the neurotoxin inducing Parkinson's disease, is a potent competitive inhibitor of human and rat cytochrome P450 isozymes (P450bufI, P450db1) catalyzing debrisoquine 4-hydroxylation. Biochem. Biophys. Res. Commun. *148:*1144–1150.

Ghersi-Egea, J.-F., R. Perrin, B. Leininger-Muller, M.-C. Grassiot, C. Jeandel, J. Floquet, G. Cuny, G. Siest, and A. Minn (1993) Subcellular localization of cytochrome P450, and activities of several enzymes responsible for drug metabolism in the human brain. Biochem. Pharmacol. *45:*647–658.

Giros, B., and M.G. Caron (1993) Molecular characterization of the dopamine transporter. Trends Pharmacol. Sci. *14:*43–49.

Gonzalez, F.J. (1989) The molecular biology of cytochrome P450s. Pharmacol. Rev. *40:*243–288.

Gonzalez, F.J., T. Matsunaga, K. Nagata, U.A. Meyer, D.W. Nebert, J. Pastewka, C.A. Kozak, J. Gillette, H.V. Gelboin, and J.P. Hardwick (1987) Debrisoquine 4-hydroxylase: Characterization of a new P450 gene subfamily, regulation, chromosomal mapping, and molecular analysis of the DA rat polymorphism. *DNA 6:*149–161.

Gonzalez, F.J., R.C. Skoda, S. Kimura, M. Umeno, U.M. Zanger, D.W. Nebert, H.V. Gelboin, J.P. Hardwick, and U.A. Meyer (1988) Characterization of the common genetic defect in humans deficient in debrisoquine metabolism. Nature *331:*442–446.

Gough, A.C., J.S. Miles, N.K. Spurr, J.E. Moss, A. Gaedigk, M. Eichelbaum, and C.R. Wolf (1990) Identification of the primary gene defect at the cytochrome P_{450} CYP2D locus. Nature *347:*773–776.

Guengerich, F. P. (1992) Human cytochrome P-450 enzymes. Life Sci. *50:*1471–1478.

Hadley, W.M., and A.R. Dahl (1982) Cytochrome P-450 dependent monooxygenase activity in rat nasal epithelial membranes. Toxicol. Lett. *10:*417–422.

Haglund, L., C. Kohler, T. Haaparanta, M. Goldstein, and J.-Å. Gustafsson (1984) Presence of NADPH-cytochrome P450 reductase in central catecholaminergic neurones. Nature *307:*259–262.

Hansson, T., N. Tindberg, M. Ingelman-Sundberg, and C. Köhler (1990) Regional distribution of ethanol-inducible cytochrome P450 IIE1 in the *rat central nervous system. Neuroscience 34:451–463.*

Hirai, M., N. Kitamura, T. Hashimoto, T. Nakai, T. Mita, O. Shirakawa, T. Yamadori, T. Amano, S.A. Noguchi-Kuno, and C. Tanaka (1988) [^{3}H]GBR-12935 binding sites in human striatal membranes: binding charateristics and changes in parkinsonians and schizophrenics. Jpn. J. Pharmacol. *47:*237–243.

Hodgson, A.V., T.B. White, J.W. White, and H.W. Strobel (1993) Expression analysis of the mixed function oxidase system in rat brain by the polymerase chain reaction. Mol. Cell. Biochem. *120:*171–179.

Hsu, S.M., L. Raine, and H. Fanger (1982) The use of avidin-biotin peroxidase complex (ABC) in immunoperoxidase techniques. A comparison between ABC and unlabeled antibody (PAP) procedure. J. Histochem. Cytochem. *29:*577–580.

Iscan, M., K. Reuhl, B. Weiss, and M.D. Maines (1990) Regional and subcellular distribution of cytochrome P-450-dependent drug metabolism in monkey brain: The olfactory bulb and the mitochondrial fraction have high levels of activity. Biochem. Biophys. Res. Commun. *169:*858–863.

Kadowaki, K., J. Kishimoto, G. Leng, and P.C. Emson (1994) Up-regulation of nitric oxide synthase (NOS) gene expression together with NOS activity in the rat hypothalamo-hypophysial system after chronic salt loading: evidence of a neuromodulatory role of nitric oxide in arginine vasopressin and oxytocin secretion. Endocrinology *134:*1011–1017.

Kapitulnik, J., H.V. Gelboin, F.P. Guengerich, and D.M. Jacobowitz (1987) Immunohistochemical localization of cytochrome P-450 in rat brain. Neuroscience *20:*829–833.

Köhler, C., L.G. Eriksson, T. Hansson, M. Warner, and J.-Å. Gustafsson (1988) Immunohistochemical localization of cytochrome P-450 in the rat brain. Neurosci Lett. *84:109–114.*

Komori, M. (1993) A novel P450 expressed at the high level in rat brain. Biochem. Biophys. Res. Commun. *196:*721–728.

Lledó, P. (1993) Variations in drug metabolism due to genetic polymorphism. A review of the debrisoquine/sparteine type. Drug Invest. *5:*19–34.

Marcusson J., and K. Eriksson (1988) [^{3}H]GBR-12935 binding to dopamine uptake sites in the human brain. Brain Res. *457:*122–129.

Nebert, D.W., D.R. Nelson, M.J. Coon, R.W. Estabrook, R. Feyereisen, Y. Fujii-Kuriyama, F.J. Gonzalez, F.P. Guengerich, I.C. Gunsalus, E.F. Johnson, J.C. Loper, R. Sato, M.R. Waterman, and D.J. Waxman (1991) The P450 gene family: Update on new sequences, gene mapping, and recommended nomenclature. DNA Cell Biol. *10:*1–14.

Nef, P., J. Heldman, D. Lazard, T. Margalit, M. Jaye, I. Hanukoglu, and D. Lancet (1989) Olfactory-specific cytochrome P-450. J. Biol. Chem. *264:*6780–6785.

Nelson, D.R., T. Kamataki, D.J. Waxman, F.P. Guengerich, R.W. Estabrook, R. Feyereisen, F.J. Gonzalez, M.J. Coon, I.C. Gunsalus, O. Gotoh, K. Okuda, and D.W. Nebert (1993) The P450 superfamily—update on new

sequences, gene-mapping, accession numbers, early trivial names of enzymes, and nomenclature. DNA Cell Biol. *12:*1–51.

Niznik, H.B., R.F. Tyndale, F.R. Sallee, F.J. Gonzalez, J.P. Hardwick, T. Inabe, and W. Kalow (1990) The dopamine transporter and cytochrome CYP2D1 (Debrisoquine 4-hydroxylase) in brain: Resolution and identification of two distinct [^{3}H]GBR-12935 binding proteins. Arch. Biochem. Biophys. *276:*424–432.

Norris, P.J., J.P. Hardwick, and P.C. Emson (1994) Localization of NADPH cytochrome P450 oxidoreductase in rat brain by immunohistochemistry and *in situ* hybridization and a comparison with the distribution of neuronal NADPH-diaphorase staining. Neuroscience *61:*331–350.

Ohta, S., O. Tachikawa, Y. Makino, Y. Tasaki, and M. Hirobe (1990) Metabolism and brain accumulation of tetrahydroisoquinoline (TIQ) a possible parkinsonism inducing substance, in an animal-model of a poor debrisoquine metabolizer. Life Sci. *46:*599–605.

Pai, K.S., and V. Ravindranath (1991) Protection and potentiation of MPTP-induced toxicity by cytochrome P-450 inhibitors and inducers: *in vitro* studies with brain slices. Brain Res. *555:*239–244.

Przuntek, H., H. Russ, K. Henning, and U. Pindur (1985) The protective effect of 1-tert, butyl-4,4-diphenylpiperidine against the nigrostriatal neurodegeneration causedby 1-methyl-4-phenyl-1,2,3,6-tetrahydropyridine. Life Sci. *37:*1195–2000.

Ravindranath, V., H.K. Anandatheerthavarada, and S.K. Shankar (1989) Xenobiotic metabolism in human brain—presence of cytochrome P-450 and associated mono-oxygenases. Brain Res. *496:*331–335.

Russ, H., H. Przuntek, K. Henning, and U. Pindur (1986) MPTP: A Neurotoxin Producing a Parkinsonian Syndrome. New York: Academic Press.

Shahi, G.S., S.M. Moochhala, E.J.D. Lee, and N.P. Das (1989) Studies on the interactions of MPTP (1-methyl-4-phenyl-1,2,3,6-tetrahydropyridine) with the cytochrome P-450 enzyme system—clues to a possible aetiological factor in Parkinson's disease. Ann. Acad. Med. *18:*93–97.

Skoda, R.C., F.J. Gonzalez, A. Demierre, and U.A. Meyer (1988) Two mutant alleles of the human cytochrome P-450db1 gene (P4502D1) associated with genetically deficient metabolism of debrisoquine and other drugs. Proc. Natl. Acad. Sci. U.S.A. *85:*5240–5243.

Smith, C.A.D., A.C. Gough, P.N. Leigh, B.A. Summers, A.E. Harding, D.M. Maranganore, S.G. Sturman, A.H.V. Schapira, A.C. Williams, N.K. Spurr, and C.R. Wolf (1992) Debrisoquine hydroxylase gene polymorphism and susceptibility to Parkinson's disease. Lancet *339:*1375–1377.

Suzuki, T., S. Fujita, S. Narimatsu, Y. Masubuchi, M. Tachibana, S. Ohta, and M. Hirobe (1992) Cytochrome P450 isozymes catayzing 4-hydroxylation of parkinsonism-related compound 1,2,3,4-tetrahydroquinoline in rat liver microsomes. FASEB J. *6:*771–776.

Swanson, L.W. (1992) Brain Maps: Structure of the Rat Brain. Amsterdam: Elsevier.

Tyndale, R.F., R. Sunahara, T. Inaba, W. Kalow, F.J. Gonzalez, and H.B. Niznik (1991) Neuronal cytochrome CYP2D1 (debrisoquine/sparteine-type): Potent inhibition of activity by (−)-cocaine and nucleotide sequence identity with human hepatic P450 gene CYP2D6. Mol. Pharmacol. *40:*63–68.

Warner, M., C. Köhler, T. Hansson, and J.-Å. Gustafsson (1988) Regional distribution of cytochrome P-450 in the rat brain: spectral quantification and contribution of P-450b,e and P-450c,d. J. Neurochem. *50:*1057–1065.